ISSN 1330-3651 (Print), ISSN 1848-6339 (Online)
Received: 4 April 2026; Accepted: 14 May 2026

https://doi.org/10.17559/TV-20260404003512
Original scientific paper

The Model of Road Roughness Detection Based on Smartphones and its Application

Jia WEI, Xiaolong ZOU*, Yujing ZHANG, Jiayue SUN, Weixiang WANG, Hongjun JING

Abstract: Given the high cost, long detection cycle, and poor universality of traditional road roughness detection methods and the lack of mature models in the existing smartphone-based detection techniques, a smartphone-based lightweight road roughness detection method was proposed in this study, aiming to achieve low-cost, efficient, and accurate measurement of road roughness. First, longitudinal acceleration data were acquired through a smartphone as the data acquisition terminal on an electric bicycle running at a constant speed, the mean value was then eliminated, and Kalman filtering preprocessing was performed for denoising; second, the maximum gap value was measured using a three-meter straightedge, and the international roughness index (IRI) was calculated as the benchmark data; subsequently, the maximum acceleration most highly correlated with IRI was screened based on the Pearson correlation analysis, and a quadratic function fitting model was established; finally, five-level pavement roughness evaluation criteria were established by analyzing such influencing factors as the installation location of the smartphone, the vehicle speed, and the road conditions, and the model's effectiveness was verified. The goodness of fit (R^2) of the model reached 0.8471, and the relative error on 30 verification road sections was kept within 20%. When applied to Zuitou Village Highway detection in Xi'an, the model could accurately distinguish "good" and "intermediate" pavements, highly matching the actual road conditions and their service life. The detection method based on smartphone accelerations, which features a low cost, convenient operation and wide coverage, renders a practical technical path for road roughness detection, especially applicable to the refined maintenance monitoring of low-grade roads like rural highways.

Keywords: acceleration; data preprocessing; international roughness index (IRI); pavement evaluation criteria; road roughness detection; rural highway; smartphone; three-meter straightedge method

1 INTRODUCTION

Road quality detection is an important means of ensuring road traffic safety. Nowadays, pavement quality has been detected by road maintenance departments mainly through professional pavement quality detection vehicles, and this method is characterized by the high cost, long detection cycle, and poor universality despite high precision. However, no mature methods have been developed to realize effective road quality detection by combining the acceleration and angular velocity sensors in smartphones. Therefore, a key problem to be urgently solved lies in efficiently conducting road quality detection and ensuring the safety of road traffic with low-cost and high-applicability advantages.

Smartphones have built-in sensors such as accelerometers, gyroscopes, and cameras, which can collect data of vehicle vibration and road photos for road quality detection. The pavement quality detection based on smartphones integrates the advantages of low cost, wide coverage, and high timeliness, becoming a research hotspot in the field of road detection. In this study, a smartphone-based pavement quality detection method was put forward, and machine learning and deep learning methods were applied to learn the pavement quality indices and the advanced features of pavement disease information based on the vehicle vibration data acquired by the vehicle-mounted smartphone and the pavement image data, achieving the lightweight detection of pavement quality.

Modern smartphones integrate a variety of sensors, which can realize the acquisition and transmission of triaxial acceleration, positioning, and velocity measurement data, along with user-friendly interface display, serving as portable devices with rich functions. Using a GIS-based intelligent road traffic quality monitoring platform and applying a smartphone as the mobile intelligent terminal for traffic data acquisition, some critical techniques in the intelligent road traffic quality evaluation method based on the traffic data perceived by smartphones were investigated through the running test, the data correlation analysis, the comparative selection of vibration indices, and the determination of the vibration threshold.

With an increasing number of built-in sensors, smartphones have been widely applied in the field of intelligent transportation, e.g., pedestrian positioning, road network establishment, and travel mode recognition. The sensors commonly applied to smartphones include motion sensors (e.g., accelerometers and gyroscopes), environmental sensors (e.g., barometers and photometers) and position sensors (e.g., magnetometers). These sensors provide a data basis for pavement quality estimation. For instance, they can indirectly identify road bumps and further evaluate road roughness by analyzing the changes in acceleration and angular velocity.

On this basis, investigating the smartphone-based road roughness detection is not only theoretically significant but also can provide road users with unblocked and safe road infrastructure. In this study, a smartphone-based road quality detection method was raised. This detection method is especially applicable to rural highways and low-grade roads, where professional detection vehicles are too costly and impractical for regular maintenance monitoring.

Specifically, road roughness results were classified based on the acceleration and angular velocity data acquired by the smartphone. The results aim to provide theoretical support and technical paths for the smartphone-based road roughness detection and render a test basis for their application in highway engineering construction.

2 STATE OF THE ART

The domestic and foreign research on smartphone-based road roughness detection and related fields have presented evident trends from single-index evaluation to multi-attribute fusion and from traditional machine learning to lightweight deep learning models in recent years. Pavement quality detection is one of the important research directions in road detection, while pothole and pavement roughness are significant indices deciding pavement quality, so many scholars have been dedicated to the research on pavement potholes and roughness. For example, pavement pothole detection methods based on

smartphone inertial sensors have been proposed. Microsoft Research India has developed two systems-Nericel and Traffic Sense [1], which can realize pavement pothole detection based on the built-in accelerometers and microphones in Windows smartphones. The above systems implement pothole detection mainly using threshold-based heuristic methods, which are of specific subjectivity since the thresholds are determined by manual observations. Wolverine et al. [2] detected road bumps or potholes according to the changes in data acquired by an accelerometer perpendicular to the ground. Using this method, the threshold was determined through the mean value and standard deviation, while neglecting high-order statistical parameters. Allouch et al. [3] classified pavement quality into two types: smooth and rough, and detected pavement quality through a machine learning method. Nuno et al. [4] applied the data mining method developed by Scikit-learn and Weka to detect rough manhole covers and potholes on the pavement. Meanwhile, pavement potholes have been detected by similar techniques in some literature [5-8] .

Additionally, some scholars have evaluated pavement quality by calculating the international roughness index (IRI) [9] of pavements. PAVEMON [10] is a GIS network-based pavement monitoring system developed by the VOTERS project, which acquires such quality parameters as pavement roughness and crack density of different roads from multiple sensors, including accelerometers, tire pressure sensors, cameras, and lidars. Nevertheless, this system, which needs special detection vehicles, is costly, restricting its application as a large-scale road detection platform.

Zhou et al. [11] focused on the systematic utilization of built-in sensors (e.g., accelerometers, gyroscopes, and barometers) in smartphones and achieved low-cost and efficient road quality detection through machine learning methods. In a paper published by them in 2023, they used the IRI acquired by professional detection vehicles [12, 13] as the true value, applied the acceleration and angular velocity data acquired by smartphones, and combined a support vector machine. Then, the average quality classification accuracy for urban roadways and expressways, respectively, reached 89.4% and 88.9%, respectively, based on the data of roads totaling 173 km in Wuhan, Hubei, and Dazhou, Sichuan, verifying the effectiveness of this model under different road types.

The smartphone-based method for extracting the slope information of pedestrian road networks fuses the data of accelerometers, barometers, and GPS, uses the slope value calculated by high-precision LiDAR data, establishes a machine learning regression model to predict the road slope, and finally updates the results into the map data, providing a data basis for personalized navigation (e.g., wheelchair users and energy-saving routes for electric bicycles) considering slope factors. In terms of road disease detection, the potential of smartphone images has been exhibited in related studies, e.g., image detection of road manhole covers based on residual network (ResNet) models, with the accuracy reaching as high as 80.97%. Besides, the subsidence degree of roads can be classified according to the acceleration data generated when a vehicle runs through manhole covers, and the classification accuracy reaches 86.0%.

Internationally, the research regarding this field has been inclined to technology fusion and practicality. For instance, a research team established a comprehensive dataset covering road anomalies and driving behaviors to promote algorithm development. Meanwhile, lightweight deep learning models (e.g., MobiLiteNet) have been raised to optimize the computational cost and realize the real-time road disease detection on smartphones. To sum up, the smartphone-based road quality detection technique is developing rapidly towards directions of multi-source data fusion, algorithm model optimization, and standardized application by virtue of low costs and favorable universality. This technique is expected to serve as an important supplement to the traditional professional detection system and provide powerful support for the refined maintenance of intelligent transportation and infrastructure.

Nowadays, smartphones are integrating an increasing number of built-in sensors to measure different information on users and their surrounding environments, so they have been extensively applied in the field of intelligent transportation, e.g., pedestrian positioning [14-16], road network establishment [17, 18], and travel mode recognition [19]. The built-in sensors of smartphones mainly include motion sensors (acceleration sensors, gravity sensors, gyroscopes, and rotation vector sensors), environmental sensors (barometers, photometers, and thermometers), and position sensors (telegoniometers and magnetometers). These sensors may render some necessary data to estimate pavement quality. For example, the road bumps can be directly reflected by the changes in acceleration and angular velocity data of smartphones, thereby detecting road roughness. In terms of vehicle-pavement dynamic interaction, Gao et al. [20] investigated the influence of pavement-tyre interface on cycling comfort, highlighting the importance of vibration transmission mechanisms for roughness detection using lightweight vehicles such as bicycles and electric bicycles. Hence, a model was established based on the vehicle acceleration acquired by the smartphone and its correlation with the international roughness index (IRI), and finally, the road conditions on Zuitou Village Highway in Xi'an were assessed through the acceleration data.

3 METHODOLOGY

3.1 Data Acquisition and Preprocessing

Smartphones (Huawei nova5 pro and Xiaomi 12) installed with MATLAB were placed on a two-wheel electric bicycle running at a constant speed of 20 km/h to acquire longitudinal acceleration data at a sampling frequency of 10 Hz.

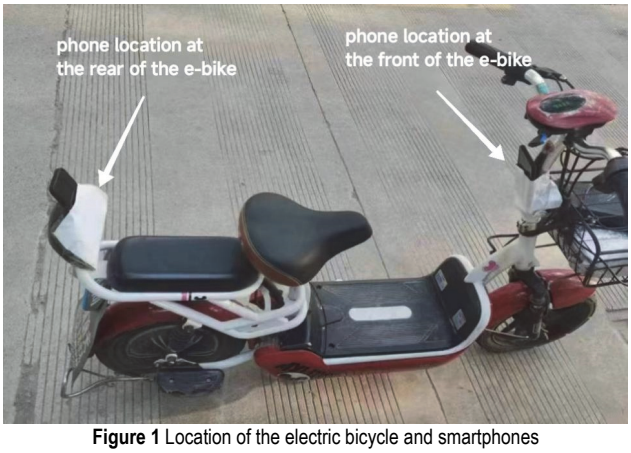

Figure 1 Location of the electric bicycle and smartphones

The road section for data acquisition covered different road conditions (smooth, aggregate exposure, faulting of slab ends, potholes, etc.). After acquisition, the original acceleration data were subject to mean value elimination and Kalman filtering to eliminate noise and low-frequency interferences and extract real pavement excitation signals, as shown in Fig. 1.

3.2 Pavement Roughness Detection through the Three-Meter Straightedge Method

To obtain the benchmark data of pavement roughness, a field measurement was performed on 30 test road sections with the three-meter straightedge method, as shown in Fig. 2.

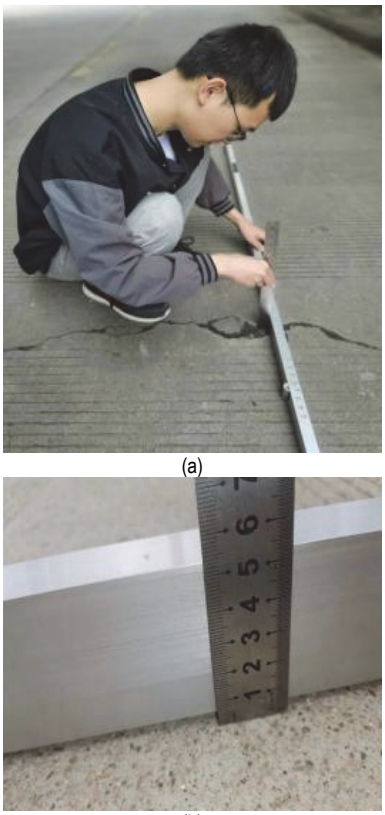

(a)

(b)

Figure 2 Pavement roughness measurement with a three-meter straightedge

Before detection, the location of the measuring point was determined at 0.9 m from the lane line in accordance with relevant specifications. Specifically, the rut center on the already rutted pavement was chosen as the measuring point, and surface sundries were cleared. Each road section was subject to the measurement for consecutive ten feet by folding and fixing a three-meter straightedge. Leveling was performed using level bubble, the maximum gap position between the straightedge and pavement was determined through visual observation, and the height of the gap was measured through a depth gauge, which was accurate to 0.1 mm.

The three-meter straightedge method is a standard procedure specified in the Chinese highway engineering regulation (JTG 3450-2019) for low-speed road sections. The conversion formula $IRI = 0.38 \times L_{max}$ has been validated in previous studies, with an error margin within ±10% compared to professional profilometers. Therefore, the IRI values derived from this method serve as reliable benchmark data for establishing the acceleration-roughness relationship model.

3.3 Pavement Roughness Index Based on Acceleration

3.3.1 Acceleration acquisition

The same electric bicycle was driven at a speed of 20 km/h to acquire the acceleration data on each road section, and IRI of each road section was synchronously collected using a three-meter straightedge. To test the stability of the vehicle vibration acceleration acquired by the smartphone, repeated tests were carried out on the same road section for the follow-up confirmatory analysis. A total of 6 road sections were selected, data acquisition was conducted 5 times on each road section, and the data collected by the smartphone were preprocessed to obtain the real longitudinal acceleration, as shown in Fig. 3.

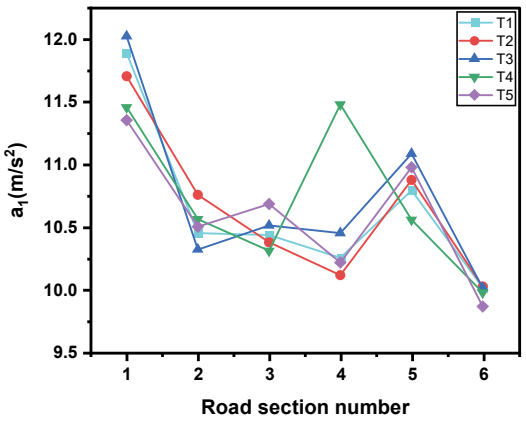

Maximum acceleration a_1 on different road sections

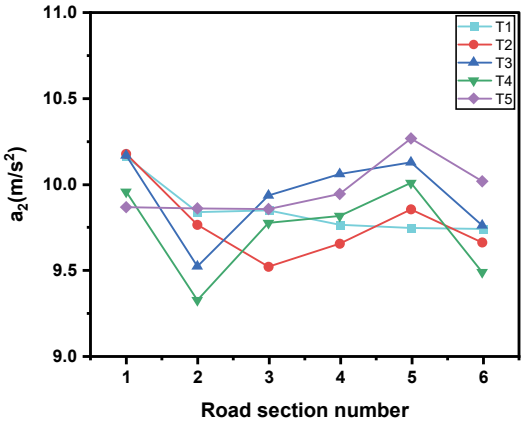

Average acceleration a_2 on different road sections

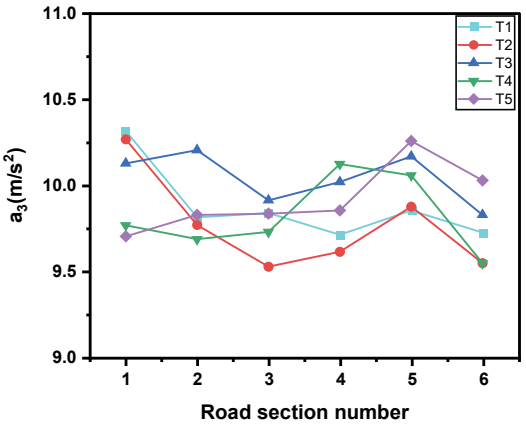

Median acceleration a_3 on different road sections

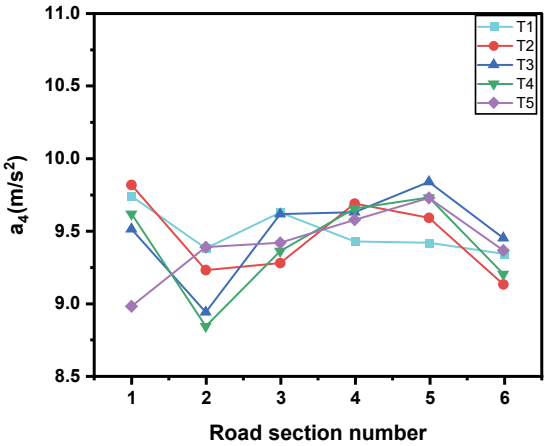

Minimum acceleration a_4 on different road sections

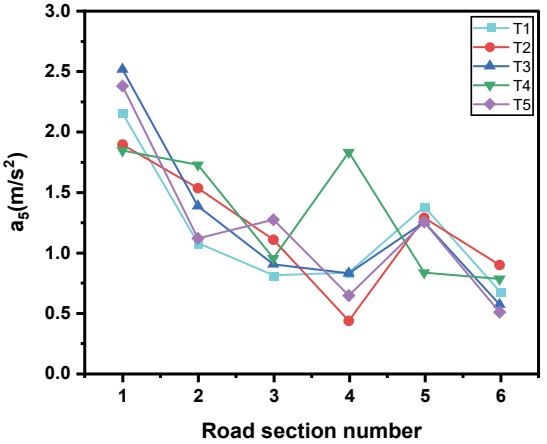

Acceleration difference a_5 on different road sections

Figure 3 Line charts of accelerations on different road sections

It could be clearly observed that the acceleration data acquired by the smartphone were relatively stable, and individual outliers were excluded from the obtained acceleration a. The acceleration (a) values were relatively concentrated on the same road section, and the a values were evidently different under different road conditions, conforming to the requirements for distinguishing different road conditions.

3.3.2 Pavement Roughness Index Model Based on Acceleration

The measured road sections were screened and divided, and the 30 sections were numbered. On each selected road section, data acquisition was performed at a speed of 20 km/h, the acquired acceleration a was preprocessed to obtain the real acceleration, and the *IRI* of each numbered road section was calculated as per $IRI = 0.3803L_{\max} - 0.4573$ according to the maximum gap measured by the three-meter straightedge. Data were sorted out, and the correlations of the maximum, average, median, and minimum accelerations with *IRI* were analyzed.

According to the measured maximum gap $L_{\max}$ and combining $IRI = 0.3803L_{\max} - 0.4573$, the *IRI* of each road section was solved, providing true and reliable benchmark data for the subsequent acceleration-roughness relationship modeling. The detection results are listed in Tab. 1. The acceleration values a_1, a_2, a_3, a_4, and a_5 obtained through preprocessing and the *IRI* values of different road sections calculated as per the formula are displayed in Tab. 2.

Table 1 Pavement roughness detection results obtained through the three-meter straightedge method

Road section No.	Maximum gap per foot after measurement for consecutive ten feet by the three-meter straightedge / mm										IRI / m/km
	1	2	3	4	5	6	7	8	9	10	
1	4.8	4.3	4.6	6.4	6.6	5.3	8.1	5.6	5.2	7.6	2.6176
2	3.9	4.8	5.4	4.8	4.1	4.6	6.3	6.1	4.4	5.8	1.9331
3	5.3	4.4	5.1	4.1	3.7	4.4	5.1	4.8	4.3	3.7	1.5528
4	6.5	7.5	5.9	6.8	5.2	8.3	5.5	7.9	4.4	6.2	2.6937
5	6.6	6.3	5.9	5.4	7.1	5.4	6.6	6.2	4.8	5.6	2.2373
6	6.2	5.7	5.6	4.8	6.5	5.0	5.2	4.7	6.1	5.5	2.0091
7	3.5	3.9	5.7	4.4	4.9	3.8	4.8	3.6	4.2	5.0	1.7049
8	4.7	4.3	6.0	4.2	6.9	6.2	3.6	5.9	5.2	4.1	2.1613
9	5.5	4.4	4.7	6.5	8.1	4.7	6.7	7.2	4.0	5.3	2.6176
10	8.3	6.5	8.2	5.0	7.5	7.7	9.1	5.4	7.7	7.9	2.9979
11	9.3	13.0	11.6	8.9	11.5	10.4	12.1	8.8	9.6	8.2	10.3757
12	3.8	4.7	5.1	4.0	3.6	5.2	5.5	4.4	4.0	3.2	1.6288
13	10.2	8.5	8.3	8.8	9.3	8.0	7.6	9.4	11.1	10.4	3.7585
14	12.9	11.9	10.4	14.7	9.8	13.2	8.8	11.6	12.3	9.2	5.1276
15	6.6	6.2	5.1	7.2	7.0	7.9	5.3	5.8	6.1	5.7	2.5416
16	4.2	5.0	5.5	3.4	3.4	4.8	5.5	4.8	3.8	4.6	1.6288
17	3.0	2.8	2.9	4.7	3.5	4.0	3.3	4.1	3.8	3.9	1.3246
18	4.6	3.4	7.3	3.1	5.3	6.2	7.7	6.9	5.9	4.9	2.4655
19	8.2	8.9	6.0	7.4	8.1	4.1	6.7	7.1	5.4	5.8	2.9219
20	7.9	4.8	6.4	3.8	4.4	5.7	6.1	5.0	7.1	7.2	2.5416
21	6.9	3.7	4.6	3.6	4.0	5.4	6.1	4.7	5.1	6.2	2.1613
22	4.7	5.4	5.7	6.3	6.1	3.7	4.3	4.9	4.4	3.4	1.9331
23	8.1	9.5	8.8	13.8	10.8	12.8	9.2	10.5	10.1	14.3	4.9755
24	3.2	5.6	4.1	4.0	4.6	3.7	6.3	5.4	4.5	5.8	1.9331
25	15.1	10.0	8.6	13.6	11.6	12.9	10.3	9.8	9.6	12.2	5.2797
26	6.7	6.2	5.7	5.5	4.5	7.1	4.0	4.9	5.4	5.3	2.2373
27	8.9	6.0	8.2	7.6	10.3	9.6	6.3	11.1	9.3	10.4	3.7585
28	7.9	9.7	9.3	8.2	8.9	7.3	6.9	6.6	5.4	4.6	3.2261
29	6.5	8.4	7.4	6.3	8.2	4.8	6.0	6.9	7.3	9.1	2.9979
30	7.6	5.1	5.8	4.5	7.8	6.5	6.9	8.5	9.3	8.8	3.0740

Table 2 Statistical table of acceleration and *IRI*

a_1	a_2	a_3	a_4	a_5
10.9813	10.3172	10.3134	9.7606	1.2207
10.7053	9.7366	9.7314	9.2282	1.4771
9.8627	9.2753	9.2718	8.8154	1.0473
10.6818	10.3345	10.3318	10.0279	0.6539
10.5158	9.8955	9.8927	9.3862	1.1296
10.3755	9.8334	9.8305	9.3959	0.9796
9.6663	9.4444	9.4432	9.1698	0.4965
10.1129	9.8656	9.8646	9.6468	0.4661
10.6379	10.2306	10.2232	9.746	0.8919
11.0334	10.2954	10.2923	9.9848	1.0486
14.8654	10.3101	10.3152	9.8652	6.6599
9.6301	9.3912	9.3912	8.8928	0.7373
12.5605	9.689	9.6748	8.9761	3.5844
15.9746	10.2703	10.2442	9.7152	6.2594
10.4209	10.2469	10.2441	10.1111	0.3098
9.1928	8.7797	8.7751	8.3832	0.8096
11.3483	8.7495	8.739	8.0774	3.2709
10.6818	10.3345	10.3318	10.0279	0.6539
12.8436	9.6687	9.6592	9.2125	3.6311
10.6062	9.9092	9.9053	9.5442	1.062
10.4856	9.7719	9.7655	9.1815	1.3041
9.9788	9.5849	9.5828	9.1453	0.8335
13.6687	9.8907	9.8702	9.5244	4.1443
10.6894	9.7069	9.7033	9.3212	1.3682
14.4643	10.1049	10.0754	9.2977	5.1666
10.4713	9.7422	9.7391	9.3451	1.1262
12.307	10.0092	9.999	9.534	2.773
11.7281	10.4332	10.4295	9.7475	1.9806
10.8532	10.0273	10.0242	9.4915	1.3617
11.1729	9.6594	9.6474	9.2831	1.8898

According to the Pearson correlation analysis method, a correlation analysis was performed on a_1, a_2, a_3, a_4, and a_5 with *IRI*, as seen in Tab. 3.

Table 3 Pearson correlation coefficients

	IRI
a_1	0.920**
a_2	0.552**
a_3	0.542**
a_4	0.421*
a_5	0.835**
$*p < 0.05$ $**p < 0.01$	

According to Tab. 3, a_1, a_2, a_3, a_4, and a_5 presented significantly positive correlations with *IRI*, where a_1 exhibited the highest correlation with *IRI*, so the correlation between the maximum acceleration and *IRI* is more suitable as the acceleration-*IRI* relational model.

The maximum acceleration a_1 and *IRI* were fitted into exponential, logarithmic, linear, and quadratic functions, and the quadratic function with the highest goodness of fit was taken as the relation between maximum value a_1 and *IRI*, as shown in Fig. 4.

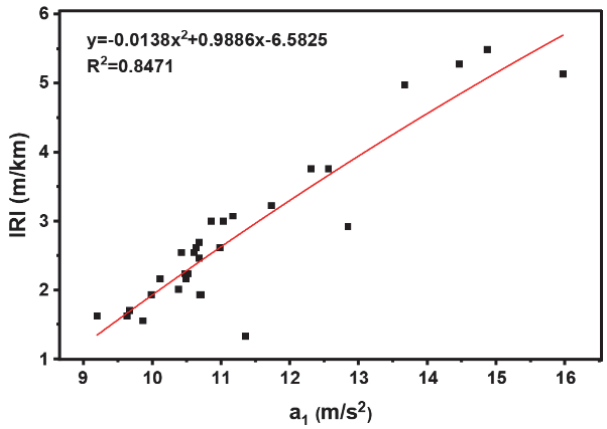

Figure 4 Distribution relationship between *IRI* and a_1

The fitting formula is:

$$y = -0.0138x^2 + 0.9886x - 6.582 \quad (1)$$

The goodness of fit is $R^2 = 0.8471$, indicating a good fitting effect and a favorable correlation.

3.3.3 Model Verification

To ensure the accuracy of the model, 30 road sections were chosen again for verification, and the preprocessed maximum acceleration a_1 was substituted into Eq. (1) to obtain the estimated *IRI* (*EIRI*), as listed in Tab. 4. and Fig. 5 is plotted.

Table 4 Error statistics of *EIRI* and actual values

Road section No.	a_1 / m/s²	*EIRI* / m/km	*IRI* / m/km	Relative error / %
1	9.7468	1.9241	1.8245	5.17
2	12.5235	3.4330	3.3457	2.54
3	10.3432	2.1691	2.4330	12.17
4	10.4544	2.2196	2.3569	6.19
5	10.2965	2.1483	1.9006	11.53
6	11.5508	2.7977	3.1175	11.43
7	9.7956	1.9425	1.6548	14.81
8	10.4101	2.1993	2.5090	14.08
9	11.0469	2.5139	3.0034	19.48
10	10.9023	2.4381	2.2809	6.45
11	16.5246	7.2562	7.07264	2.53
12	14.5822	5.1570	5.0951	1.20
13	9.6177	1.8767	1.6273	13.29
14	10.1315	2.0772	2.2048	6.14
15	9.9804	2.0149	2.0527	1.88
16	10.2175	2.1139	2.3569	11.50
17	11.3525	2.6823	2.7372	2.05
18	13.5263	4.2084	4.3345	3.00
19	10.4125	2.2004	2.5851	17.48
20	12.0563	3.1135	3.6880	18.45
21	10.4509	2.2180	2.2809	2.84
22	10.2351	2.1215	1.9724	7.03
23	9.8836	1.9764	1.7442	11.75
24	10.6578	2.3158	2.6612	14.91
25	11.5863	2.8189	2.7372	2.90
26	10.8858	2.4296	2.8133	15.79
27	15.4532	6.0416	7.0726	17.07
28	10.5863	2.2814	2.0245	11.26
29	11.6134	2.8351	2.8133	0.77
30	12.1140	3.1515	3.6119	14.61

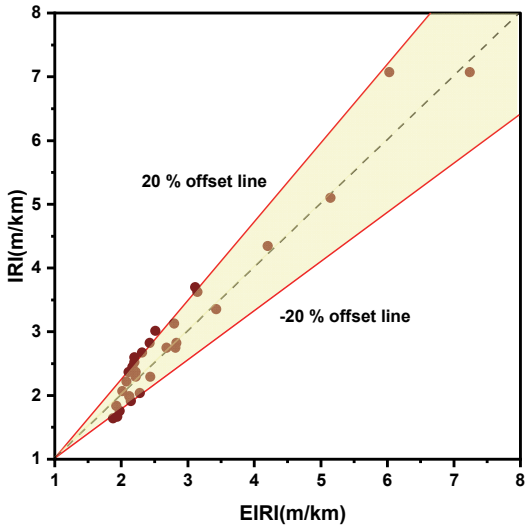

Figure 5 Comparison of *EIRI* (model calculated value) and *IRI* (three-meter straightedge measured value)

As revealed by the data analysis of 30 road sections, despite the relative error between *EIRI* and *IRI*, the overall relative error was within 20%, basically meeting the large-scale measurement requirements for low-grade roads.

The linear regression relationship between acceleration and *IRI* is determined as follows:

$$I = -0.0138a^2 + 0.9886a - 6.582 \quad (2)$$

3.3.4 Influencing Factor Analysis

The vibration generated when the vehicle ran would be transmitted by the tire to the mechanical connection and then to the smartphone, making it necessary to analyze the influence of different locations of the electric vehicle on data acquisition. Therefore, it is necessary to analyze whether the data acquisition is affected when the smartphone is placed beside the instrument panel or at the backrest of the rear seat.

A total of 18 road sections were selected, numbered, and subject to data acquisition, respectively. The acquired acceleration data were preprocessed, and *EIRI* was calculated. Fig. 6 and Fig. 7 are plotted according to the obtained data.

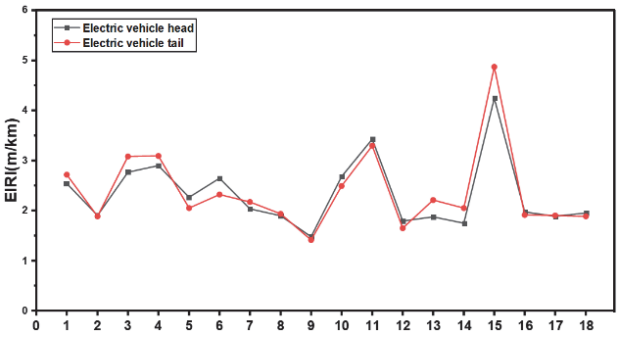

Figure 6 Broken line graph for *EIRI* at the vehicle head and tail

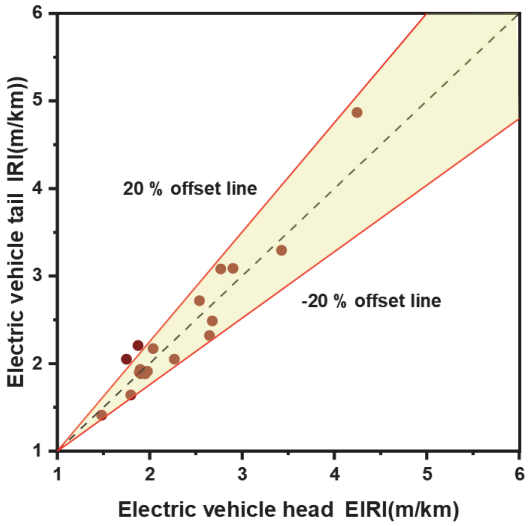

Figure 6 Comparison of *EIRI* data at the vehicle head and tail

It could be evidently seen that the relative error of *EIRI* resulting from the installation position of the smartphone was kept within 20%, conforming to requirements, so the acceleration was affected little by the installation position of the smartphone.

(2) Influence of vehicle speed

To observe the impact of the electric vehicle's speed on the measured acceleration more intuitively, a total of 16 road sections was selected, and data acquisition was performed on each road section at speeds of 30, 20, and 10 km/h. The acquired acceleration was preprocessed to calculate *EIRI*, the data acquired by the three-meter straightedge, and *IRI* was solved as per the formula. Fig. 8 and Fig. 9 were plotted according to the obtained data.

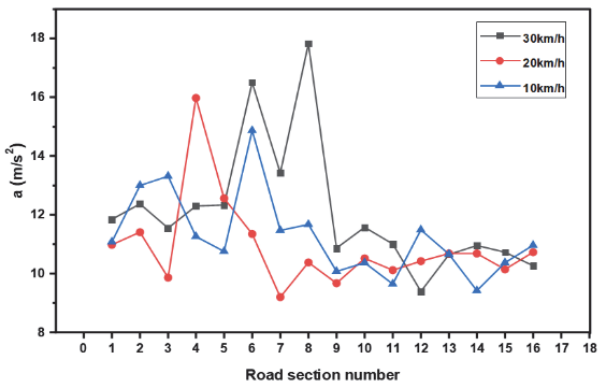

Figure 7 Broken line graph of acceleration measured at different speeds

Obvious differences were observed in the acceleration values acquired at different running speeds of the electric vehicle. All data in Section 3.3 were measured at the speed of 20 km/h, so Eq. (1) exhibited a good fitting effect at this speed.

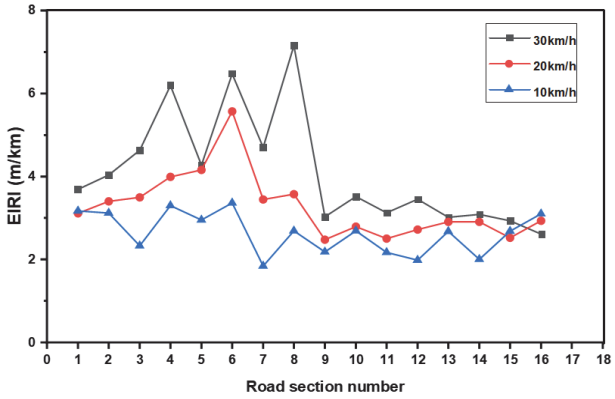

Figure 8 Broken line graph of *EIRI* measured at different speeds

(3) Influence of road conditions

To enhance the accuracy of the pavement roughness evaluation model based on acceleration, 8 smooth road sections, 8 road sections with aggregate exposure, 8 road sections with faulting of slab ends, and 8 road sections with potholes were selected, followed by data acquisition on each road section. The acquired acceleration data were preprocessed, *EIRI* was calculated, *IRI* was calculated as per the formula based on the data acquired by the three-meter straightedge, and the relative error between *IRI* and *EIRI* was calculated. The data are listed in Tab. 5. According to the data in Tab. 5, all relative errors were within 20%, meeting requirements, so Eq. (2) applies to different road conditions.

Table 5 Comparison between *RIRI* and *IRI* on different road sections

Road section No.		*EIRI* / m/km	*IRI* / m/km	Relative error / %
Smooth road section	1	2.1521	2.5203	14.61
	2	2.0254	1.9853	2.02
	3	2.1985	2.2542	2.47
	4	1.9851	1.8542	7.06
	5	1.8658	2.1521	13.30
	6	2.2542	2.6552	15.10
	7	2.3584	2.0585	14.57
	8	2.3948	2.8545	16.10
Road section with aggregate exposure	1	2.6582	2.8547	6.88
	2	3.1524	3.5482	11.15
	3	2.9458	3.0954	4.83
	4	2.7857	2.9765	6.41
	5	2.8145	3.0584	7.97
	6	3.1864	3.3548	5.02
	7	2.6640	2.8011	4.89
	8	2.9674	2.8644	3.60
Road section with faulting of slab ends	1	5.0685	5.5821	9.20
	2	4.7564	4.7732	0.35
	3	3.8021	4.0258	5.56
	4	4.9487	4.6895	5.53
	5	5.0568	5.3856	6.11
	6	4.6896	4.7684	1.65
	7	4.9741	5.2687	5.59
	8	4.8645	4.9931	2.58
Road section with potholes	1	6.8542	6.5986	3.87
	2	6.7524	7.01524	3.75
	3	7.3524	6.6842	10.00
	4	7.2584	7.5865	4.32
	5	6.4582	6.5842	1.91
	6	6.8567	7.4852	8.40
	7	7.0584	6.8421	3.16
	8	7.7585	8.5422	9.17

4 RESULT ANALYSIS AND DISCUSSION

4.1 Research on an Acceleration-Based Pavement Roughness Evaluation Method

4.1.1 Acceleration-Based Pavement Roughness Evaluation Method

At present, pavement roughness is evaluated in accordance with the *Highway Performance Assessment Standards*, as seen in Tab. 6 below.

Table 6 Evaluation criteria for pavement roughness

Technical grade	Superior	Good	Intermediate	Inferior	Poor
RQI	≥ 90	≥ 80, < 90	≥ 70, < 80	≥ 60, < 70	< 60
Bumping degree	No bumps, the vehicle runs steadily	Slightly bumpy, the vehicle runs still steadily	Obviously bumpy, the vehicle runs unstably	Seriously bumpy, the vehicle runs quite unstably	Very bympy, the vehicle runs very unstably

The pavement roughness detection data were saved for a long term with 100 m (manual detection) or 20 m (quick detection) as the unit. *RQI* is the riding quality index, which is applied to evaluate the pavement roughness as per the following formula:

$$RQI = \frac{100}{1+\alpha_0 e^{\alpha_1 IRI}} \tag{3}$$

where: *IRI* - international roughness index; α_0 - taken as 0.026 for expressways and first-class highways and 0.0185 for highways of other classes; α_1 - taken as 0.65 for expressways and first-class highways and 0.58 for highways of other classes.

By reference to the existing evaluation criteria and formulas, the acceleration-based evaluation criteria for pavement roughness were established through the calculated IRI and acceleration a, as seen in Tab. 7 below.

Table 7 Acceleration-based evaluation criteria for pavement roughness

Technical grade	Superior	Good	Intermediate	Inferior	Poor
RQI	≥ 90	≥ 80, < 90	≥ 70, < 80	≥ 60, < 70	< 60
IRI	≤ 3.0909	>3.0909, ≤ 4.4891	> 4.4891, ≤ 5.4184	> 5.4184, ≤ 6.1802	> 6.1802
a	≤ 10.9539	> 10.9539, ≤ 13.0824	> 13.0824, ≤ 14.6149	> 14.6149, ≤ 15.9593	> 15.3847
Bumping degree	No bumps, the vehicle runs steadily	Slightly bumpy, the vehicle runs still steadily	Obviously bumpy, the vehicle runs unstably	Seriously bumpy, the vehicle runs quite unstably	Very bumpy, the vehicle runs very unstably

4.1.2 Verification of the Acceleration-Based Pavement Roughness Evaluation Method

Based on the conclusions in Section 4.1, the pavement roughness level was directly evaluated through the field-measured acceleration value. To verify the accuracy of the acceleration-based evaluation criteria for pavement roughness, 20 road sections were re-selected for verification. The measured acceleration a, the *RQI* value calculated through the gap height measured by the three-meter straightedge, and the pavement grade evaluated based on the two are listed in Tab. 8. It can be seen that the acceleration-based evaluation criteria for pavement roughness meet the requirements.

Table 8 Verification of evaluation criteria

Road section No.	Acceleration / m/s^2	Road section grade	*RQI*	Road section grade
1	12.7297	Good	84	Good
2	11.4256	Good	88	Good
3	9.9674	Superior	94	Superior
4	13.6613	Intermediate	77	Intermediate
5	12.3571	Good	86	Good
6	10.9133	Superior	93	Superior
7	9.8023	Superior	94	Superior
8	12.5434	Good	85	Good
9	12.6832	Good	84	Good
10	11.9845	Good	88	Good
11	12.1708	Good	87	Good
12	12.3571	Good	86	Good
13	13.0092	Good	82	Good
14	11.5188	Good	87	Good
15	12.8229	Good	83	Good
16	13.5216	Intermediate	78	Intermediate
17	9.9485	Superior	94	Superior
18	12.9626	Good	82	Good
19	10.8201	Superior	93	Superior
20	13.1024	Intermediate	79	Intermediate

4.2 Roughness Evaluation of Zuitou Village Highway

4.2.1 Pavement Investigation of Zuitou Village Highway

In this study, the actual pavement conditions of Zuitou Village in Xi'an were investigated under the leadership of Xi'an University of Science and Technology and Zuitou Village Government in Chang'an District, Xi'an City, and the co-guidance of the school and the relevant personnel from Mingdu Street in Chang'an District. The current situation of this highway was understood by field surveys, interviews, etc., providing data support. The planar graph of Zuitou Village in Chang'an District is displayed in Fig. 9 below.

Figure 9 Planar graph of Zuitou Village in Chang'an District

The disease investigation results of the concrete pavement in Zuitou County manifest that the concrete pavement goes through plate breakage, fracture, slab corner cracking, peeling, and potholes, which may be attributed to design defects and ineffective maintenance management, as shown in Fig. 10.

(a)

(b)

Figure 10 Road conditions in Zuitou Village

4.2.2 Pavement Roughness Evaluation of Zuitou Village

In Zuitou Village, Chang'an District, five lines were selected, each line was 2000 meters long, and every 200 m of each line constituted 1 road section. For the same electric bicycle, the acceleration data of each road section were acquired at a speed of 20 km/h.

Table 9 Acceleration-based pavement roughness evaluation of Zuitou Village

Line No.	Road section No.	a / m/s^2	Pavement grade	Road section No.	a / m/s^2	Pavement grade
Line 1	1	13.8300	Intermediate	6	13.3972	Intermediate
	2	14.2337	Intermediate	7	13.6753	Intermediate
	3	13.7143	Intermediate	8	13.7917	Intermediate
	4	13.9815	Intermediate	9	13.3567	Intermediate
	5	14.1505	Intermediate	10	13.5176	Intermediate
Line 2	1	12.7695	Good	6	12.6311	Good
	2	12.3996	Good	7	11.4490	Good
	3	11.4028	Good	8	12.7695	Good
	4	11.6662	Good	9	12.8084	Good
	5	11.1666	Good	10	12.7644	Good
Line 3	1	13.5968	Intermediate	6	13.3972	Intermediate
	2	13.7531	Intermediate	7	13.9386	Intermediate
	3	13.3158	Intermediate	8	13.6753	Intermediate
	4	14.2241	Intermediate	9	13.2748	Intermediate
	5	13.5968	Intermediate	10	13.8300	Intermediate
Line 4	1	14.0939	Intermediate	6	14.1678	Intermediate
	2	13.4411	Intermediate	7	13.9442	Intermediate
	3	13.4215	Intermediate	8	13.5281	Intermediate
	4	14.1310	Intermediate	9	13.9818	Intermediate
	5	13.7477	Intermediate	10	14.2858	Intermediate
Line 5	1	12.7695	Good	6	11.8300	Good
	2	11.4028	Good	7	11.3093	Good
	3	12.7203	Good	8	12.4028	Good
	4	12.5610	Good	9	11.5860	Good
	5	11.8521	Good	10	12.0624	Good

The results after data processing in Section 4.2.1 are listed in Tab. 9, and the pavement grade was analyzed. In this section, the pavement of Zuitou Village will be manually evaluated through the measured acceleration.

It can be seen from Tab. 9 that the pavements of Lines 2 and 5 are evaluated as "good"; those of Lines 1, 3, and 4 are evaluated as "intermediate". It is known through interviews that Lines 2 and 5 are newly built within five years, with relatively shorter service time and lower pavement damage degree. Lines 1 and 4 have been completed for about 8-10 years, already subject to such diseases as plate breakage, slab corner cracking, and potholes. According to relevant standards, a highway evaluated as "intermediate", "inferior", or "poor" should accept damage treatment and maintenance, and the maintenance frequency should be elevated so that the highway can exert normal functions. After maintenance, the highway should be re-evaluated, and routine maintenance cannot be recovered until its grade becomes good or superior.

5 CONCLUSION

In this study, a relational model between the vehicle acceleration acquired by the smartphone and IRI was established and verified. Finally, the pavement conditions of Zuitou Village in Xi'an City were evaluated through the acceleration data, and the following conclusions were drawn:

(1) Through the theoretical analysis, an acceleration-based pavement roughness evaluation model - $y = -0.0138x^2 + 0.9886x - 6.582$ - was evaluated with the maximum acceleration as the index based on the maximum value, minimum value, mean value, median, and difference of longitudinal acceleration, and its accuracy was verified.

(2) The influencing factors of the model were analyzed, where the model was affected little by the installation position of the smartphone and different road conditions, but it was greatly influenced by the vehicle speed. A good fitting effect was achieved at the vehicle speed of 20 km/h.

(3) The acceleration-based evaluation criteria for pavement roughness were established. With the acceleration values 10.9539, 13.0824, 14.6149, and 15.9593 m/s^2 as the demarcation points, pavement roughness was divided into five levels: superior, good, intermediate, inferior, and poor, and the evaluation criteria were verified.

(4) The pavement conditions of Zuitou Village were evaluated through the acceleration-based pavement roughness evaluation method. The pavement grade of this village was evaluated as intermediate on the whole, and the evaluation method achieved a good application effect in rural highways.

The detection method based on smartphone accelerations, featuring low cost, convenient operation, and wide coverage, provides a practical technical path for road roughness detection, particularly for the refined maintenance monitoring of rural highways and low-grade roads.

Acknowledgements

This research was supported by the Natural Science Basic Research Program of Shaanxi (Grant No. 2024J-

YBMS-297), Shaanxi Province's Key Research and Development Plan for 2025 (2025SF-YBXM-066), Industrialization Cultivation Project of Shaanxi Provincial Department of Education (Grant No.: 25JC070), Ankang Science and Technology Program Project: AK2025-GY-32. This research was supported by the field support from Zuitou Village Government of Chang'an District, Xi'an City.

6 REFERENCES

[1] Mohan, P., Padmanabhan, V. N. & Ramjee R. (2008). *TrafficSense: rich monitoring of road and traffic conditions using mobile smartphones*.

[2] Bhoraskar, R., Vankadhara, N., Raman, B., & Kulkarni, P. (2012). Wolverine: traffic and road condition estimation using smartphone sensors. *2012 Fourth International Conference on Communication Systems and Networks*, 1-6. https://doi.org/10.1109/COMSNETS.2012.6151382

[3] Allouch, A., Koubâa, A., Abbes, T., & Ammar, A. (2017). RoadSense: smartphone application to estimate road conditions using accelerometer and gyroscope. *IEEE Sensors Journal*, *17*(13), 4231-4238. https://doi.org 10.1109/JSEN.2017.2702739

[4] Silva, N., Soares, J., Shah, V., Santos, M. Y., & Rodrigues, H. Anomaly detection in roads with a data mining approach. *Procedia Computer Science*, *121*, 415-422. https://doi.org/10.1016/j.procs.2017.11.056

[5] Chen, K., Lu, M., Fan, X., Wei, M., & Wu, J. (2011). Road condition monitoring using on-board three-axis accelerometer and GPS sensor. *2011 6th International ICST Conference on Communications and Networking in China*, 1032-1037. https://doi.org/10.1109/ ChinaCom.2011.6158308

[6] Douangphachanh, V. & Oneyama, H. (2014). A model for the estimation of road roughness condition from sensor data collected by android smartphones. *Journal of Japan Society of Civil Engineers*, *70*(5), 103-111. https://doi.org/10.2208/jscejipm.70.I_103

[7] Seraj, F., Zwaag, B. J. V. D., Dilo, A., Luarasi, T., & Havinga, P. (2016). RoADS: a road pavement monitoring system for anomaly detection using smart phones. - içinde. *International workshop on mining ubiquitous and social environments, sunulmuş bildiri*.

[8] Singh, G., Bansal, D., Sofat, S., & Aggarwal, N. (2017). Smart patrolling: an efficient road surface monitoring using smartphone sensors and crowdsourcing. *Pervasive and Mobile Computing*, *40*, 71-88. https://doi.org/10.1016/j.pmcj.2017.06.002

[9] Sayers, M. W. & Karamihas, S. M. (1998). *The little book of profiling: basic information about measuring and interpreting road profiles*. Transportation Research Institute.

[10] Shamsabadi, S. S., Wang, M., & Birken, R. (2014). Pavemon: a gis-based data management system for pavement monitoring based on large amounts of near-surface geophysical sensor data (s. cp). *27th Annual Symposium on the Application of Geophysics to Engineering and Environmental Problems (SAGEEP), sunulmuş bildiri, European Association of Geoscientists & Engineers*. https://doi.org/10.3997/2214-4609-pdb.400.61

[11] Du, Y., Liu, C., & Li, Y. (2018). Velocity control strategies to improve automated vehicle driving comfort. *IEEE Intelligent Transportation Systems Magazine*, *10*(1), 8-18. https://doi.org/10.1109/ MITS.2017.2776148

[12] Wang, X. & Ma, B. (2013). Intelligent road detection system. *Surveying Geographic Information*, *38*(2), 74-78. https://doi.org/10.14188/j.2095-6045.2013.02.009

[13] Zhou, Y. & Guo, R. (2019). Road comprehensive inspection vehicle based on 3d technology. *Highway Engineering*, *44*(3), 61-64. https://doi.org/10.19782/j.cnki.1674-0610.2019.03.011

[14] Liu, X., Zhou, B., Huang, P., Xue, W., Li, Q., Zhu, J., & Qiu, L. (2021). Kalman filter-based data fusion of wi-fi rtt and pdr for indoor localization. *IEEE Sensors Journal*, *21*(6), 8479-8490. https://doi.org/10.1109/JSEN.2021.3050456

[15] Zhou, B., Li, Q., Mao, Q., Tu, W. & Zhang, X. (2015). Activity sequence-based indoor pedestrian localization using smartphones. *IEEE Transactions on Human-Machine Systems*, *45*(5), 562-574. https://doi.org/10.1109/THMS.2014.2368092

[16] Zhou, B., Li, Q., Mao, Q., & Zhang, X. (2014). Indoor pedestrian positioning assisted by user behavior perception. *Journal of Wuhan University (Information Science Edition)*, (6), 719-723.

[17] Zhou, B., Ma, W., Li, Q., El-Sheimy, N., Mao, Q., Li, Y., Gu, F., Huang, L., & Zhu, J. (2021). Crowdsourcing-based indoor mapping using smartphones: a survey. *ISPRS Journal of Photogrammetry and Remote Sensing*, *177*, 131-146. https://doi.org/10.1016/j.isprsjprs.2021.05.006

[18] Zhou, B., Zheng, T., Huang, J., Zhang, Y., Tu, W., Li, Q., & Deng, M. (2021). A pedestrian network construction system based on crowdsourced walking trajectories. *IEEE Internet of Things Journal*, *8*(9), 7203-7213. https://doi.org/10.1109/JIOT.2020.3038445

[19] Liang, X., Zhang, Y., Wang, G., & Xu, S. (2020). A deep learning model for transportation mode detection based on smartphone sensing data. *IEEE Transactions on Intelligent Transportation Systems*, *21*(12), 5223-5235. https://doi.org/10.1109/TITS.2019.2951165

[20] Gao, J., Sha, A., Huang, Y., Liu, Z., Hu, L., Jiang, W., Yun, D., Tong, Z., & Wang, Z. (2019). Cycling comfort on asphalt pavement: influence of the pavement-tyre interface on vibration. *Journal of Cleaner Production*, *223*, 323-341. https://doi.org/10.1016/j.jclepro.2019.03.153

Contact information:

Jia WEI, Associate Professor
Shaanxi University of Science and Technology,
No. 43 Taihua North Road, Weiyang District, Shaanxi Province, China
E-mail: 1662972823@qq.com

Xiaolong ZOU, Associate Professor
(Corresponding author)
Xi'an University of Science and Technology
No. 58 Yanta Middle Road, Beilin District, Xi'an City, Shaanxi Province, China
E-mail: zouxiaolong_1234@163.com

Yujing ZHANG, Master
Xi'an University of Science and Technology,
No. 58 Yanta Middle Road, Beilin District, Xi'an City, Shaanxi Province, China
E-mail: 25204228098@stu.xust.edu.cn

Jiayue SUN, Master
Xi'an University of Science and Technology,
No. 58 Yanta Middle Road, Beilin District, Xi'an City, Shaanxi Province, China
E-mail: 24204228057@stu.xust.edu.cn

Weixiang WANG, Engineer
The Fifth Company of China Railway First Group,
No. 58 Yanta Middle Road, Beilin District, Xi'an City, Shaanxi Province, China
E-mail: 120936853@qq.com

Hongjun JING, Professor
Xi'an University of Science and Technology,
No. 58 Yanta Middle Road, Beilin District, Xi'an City, Shaanxi Province, China
E-mail: 424689213@qq.com